Reprinted from *J. Mol. Biol.* (1994) **236**, 1262–1265

Crystals of a Fragment of Influenza Haemagglutinin in the Low pH Induced Conformation

P. A. Bullough, F. M. Hughson, A. C. Treharne, R. W. H. Ruigrok
J. J. Skehel and D. C. Wiley

J. Mol. Biol. (1994) 236, 1262–1265

Crystals of a Fragment of Influenza Haemagglutinin in the Low pH Induced Conformation

P. A. Bullough[1], F. M. Hughson[1,2], A. C. Treharne[1], R. W. H. Ruigrok[3]†
J. J. Skehel[3] and D. C. Wiley[1,2]

[1]*Department of Biochemistry and Molecular Biology and*
[2]*Howard Hughes Medical Institute, Harvard University*
7 Divinity Avenue, Cambridge, MA 02138, U.S.A.

[3]*National Institute for Medical Research*
The Ridgeway, Mill Hill, London NW7 1AA, U.K.

Fusion of the influenza viral membrane with the membrane of the host cell is preceded by a low pH induced conformation change in the viral haemagglutinin. A fragment, consisting of much of the stem domain of influenza haemagglutinin in the low pH induced conformation, has been crystallized by the vapour diffusion method. Several crystal forms have been obtained and the molecular packing in these crystals is discussed. Crystals suitable for the recording of high angle X-ray diffraction data grow in space group $C222_1$. Diffraction data have been recorded from crystals cooled to −170°C in a cryoprotectant buffer.

Keywords: haemagglutinin; crystallization; influenza; fusion; cryocrystallography

Influenza virus haemagglutinins (HA‡) have two functions in virus replication (Wiley & Skehel, 1987). They bind virus to sialylated cell surface receptors and, following endocytosis of virus-receptor complexes, they mediate the fusion of viral and endosomal membranes required for entry of the virus genome and transcriptase into the cell. The latter function, membrane fusion, is activated at the low pH of endosomes (Maeda & Ohnshi, 1980; Huang *et al.*, 1981; White *et al.*, 1981) and the process of activation involves changes in HA structure (Skehel *et al.*, 1982; Daniels *et al.*, 1983, 1985; Webster *et al.*, 1983; Yewdell *et al.*, 1983; Doms *et al.*, 1985; Jackson & Nestorowicz, 1985; White & Wilson, 1987; Godley *et al.*, 1992). We are investigating the nature of these changes and their importance for the mechanism of membrane fusion.

HA is a trimer (molecular mass 220 kDa) of identical subunits, each subunit consisting of two disulphide-linked polypeptides, HA1 and HA2. The HA1 chain of each monomer forms a globular domain distal to the viral membrane. The three HA2 chains form the transmembrane anchor, and along with segments of the three HA1 chains form a stem domain projecting from the virus surface (Wilson *et al.*, 1981). Two of the properties of HA in the fusion activated conformation have been particularly important for structural studies. First, soluble HA released from viruses by bromelain digestion (BHA), which has been useful in crystal structure analyses of native HA (Wiley and Skehel, 1977; Wilson *et al.*, 1981), aggregates at the pH of fusion to form protein micelles. This aggregated protein is unsuitable for crystallization. Secondly, BHA in such micelles is susceptible to proteolysis. We have taken advantage of this second property to prepare fragments of the stem domain of HA in the low pH conformation suitable for crystallographic analyses. Specifically we have removed HA1 residues 28 to 328 from the aggregated trimers by digestion with trypsin (Skehel *et al.*, 1982) and then isolated soluble trimeric fragments from the remaining aggregate by thermolytic removal of HA2 residues 1 to 37 (Daniels *et al.*, 1983; Ruigrok *et al.*, 1988). We report here the crystallization of this HA fragment which we call TBHA2 (for "thermolysin BHA2").

Soluble TBHA2 was purified as described (Ruigrok *et al.*, 1988) and concentrated to 8 to 15 mg/ml in PBS (10 mM phosphate buffer, 150 mM NaCl, 0·01% sodium azide, 1 mM EDTA, pH adjusted to 5·0 with 0·1 M citric acid). Crystals were grown from hanging drops by the vapour diffusion method using 24-well tissue culture plates. Crystals grew under a variety of conditions (Table 1). Type III and type IV crystals were discovered using the "incomplete factorial search" method (Carter &

† Present address: EMBL Grenoble Outstation, c/o ILL, BP 156, 38042 Grenoble Cédex 9, France.

‡ Abbreviations used: HA, influenza virus haemagglutinin; BHA, bromelain digestion; TBHA2, thermolysin BHA2.

0022–2836/94/091262–04 $08.00/0

Table 1
Crystal growth conditions

Type	Well solution	Morphology	Space group	Unit cell (Å)	Diffraction limit (Å)
I	55 to 65% saturated ammonium sulphate, 16 mM sodium citrate, pH 6·0	hexagonal prisms, plates, needles	$P3$	$a=258·6$ $c=47·2$	7·5–4·5
II	1·24 to 1·36 M sodium citrate, pH 6·0	hexagonal prisms, plates, needles	$P3$	$a=259·5$ $c=47·2$	7·5–6·0
III	2·0 M sodium potassium phosphate, 0·2 M ammonium sulphate, 0·1 M Hepes, pH 7·5	hexagonal prisms	$P3$	$a=261·8$ $c=49·3$	5·0
IV†	55 to 65% saturated ammonium sulphate, 0·1 M ADA, pH 6·5	orthorhombic bipyramids, lozenges	$C222_1$	$a=168·7$ $b=231·7$ $c=53·8$	2·2

† Data are from frozen crystals.

Carter, 1979; Jancarik & Kim, 1991). Types I, II and III crystals had an average size of 150 μm × 150 μm × 300 μm with maximum dimensions of 300 μm × 300 μm × 2000 μm. Type IV crystals had average dimensions of 300 μm × 300 μm × 300 μm with maximum dimensions of 500 μm × 500 μm × 500 μm. Crystals were harvested into well solution for diffraction studies at room temperature, and mounted in 1·5 mm glass or quartz capillaries. Space groups of crystals types I to III were determined from precession photographs recorded on film. Space group of type IV crystals was determined from data collected on a Xentronics area detector and processed with the BUDDHA software package (Durbin *et al.*, 1986; Blum *et al.*, 1987).

Type IV crystals were also examined at low temperature (−170°C) in order to increase crystal lifetime in the X-ray beam (Haas & Rossman, 1970; Petsko, 1975; Hope, 1988, 1990; Henderson, 1990). This also led to an increase in the effective resolution of diffraction. Crystals were harvested into a buffer of 65% saturated ammonium sulphate, 0·1 M ADA (*N*-(2-acetamido)iminodiacetic acid; pH 6·5). Harvested crystals were serially transferred into harvest solutions containing in addition increasing concentrations of glycerol as cryo-protectant (from 5% to 20% (v/v), 5% steps, 30 min per step). Soaked crystals were mounted in gold wire (40 μ cross-section) loops of 1 mm diameter (Teng, 1990; Gamblin & Rodgers, 1993) and placed in a nitrogen stream at −165 to −170°C. High resolution data were recorded at the Cornell High Energy Synchrotron Source on phosphor image plates. Exposed image plates were digitized with a Fuji scanner and the digitized diffraction patterns processed with the program DENZO (Z. Otwinowski, personal communication).

Patterson maps for type III and type IV crystals are shown in Figures 1 and 2. Only type IV crystals diffract well enough for high resolution structural analysis (Table 1). The Patterson maps for both types of crystal are highly featured and give an indication of the orientation of the molecules in the unit cell. The Patterson projection map for type III crystals (Figure 1) shows prominent vectors

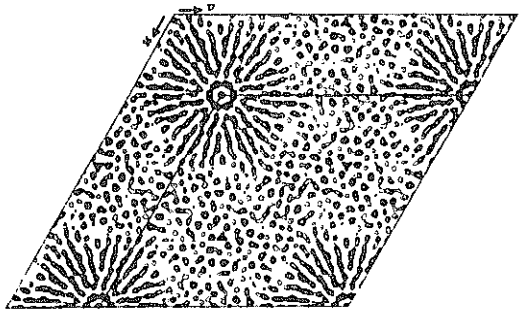

Figure 1. Patterson projection calculated from type III crystal at 5 Å resolution. The projection is down w and 1 unit cell is shown. Contours are drawn at intervals corresponding to 0·5 × root-mean-square (r.m.s.) value of the projection Patterson density. Contours start at 0·5 × r.m.s. above mean density.

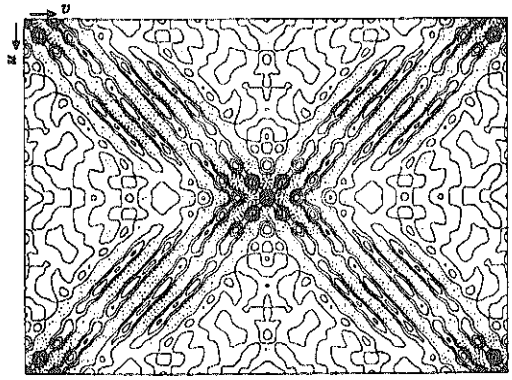

Figure 2. Patterson projection calculated from type IV crystal at 5 Å resolution. The projection is down w and 1 unit cell is shown. Contours are drawn at intervals corresponding to 1 × r.m.s. density of the projection Patterson density. Contours below the mean are broken lines.

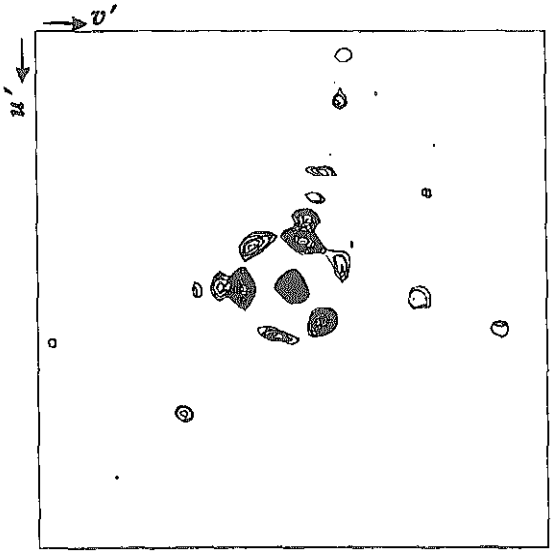

Figure 3. Sections of the Patterson map calculated for the type IV crystals at 5 Å resolution and skewed to view down the non-crystallographic 3-fold symmetry axis. Sections at a perpendicular distance of approximately 2, 3 and 4 Å from the origin are overlaid. Contours are as for Figure 2 starting at 2 × r.m.s. density above mean. The length of the u' axis is 116 Å.

diverging radially from the origin with a maximum length (in projection) of about 90 Å. In the three-dimensional Patterson map these vectors are inclined at an angle of about 25° from the u–v plane with a maximum length of about 100 Å. Such vectors probably run in a direction parallel to the α-helical structure which is known to make up a large part of TBHA2 (Ruigrok *et al.*, 1988). From electron microscopy studies we expect the TBHA2 trimer to be a rod-like molecule approximately 110 Å in length (Ruigrok *et al.*, 1988). Given that the prominent vectors in the Patterson map have a maximum length of about 100 Å we expect that these correspond to vectors along the long dimension of the trimer which will then lie about 25° from the a–b plane. The volume of the type III crystal unit cell is $2{\cdot}9 \times 10^6$ Å^3; assuming a crystal volume per unit molecular mass of between 1·68 and 3·53 Å^3/Dalton (Matthews, 1968) and a trimer molecular mass of 60 kDa, this suggests between four and nine trimers per asymmetric unit.

The projection Patterson for the type IV crystals (Figure 2) shows prominent streaks similar to those seen in Figure 1. The streaks are up to 100 Å long in the three-dimensional Patterson map and are inclined approximately 30° from the u–v plane. The volume of the unit cell is 2·1 Å^3, suggesting one to three trimers per asymmetric unit. Projection of the Patterson map in a direction approximately perpendicular to the long axis of the prominent streaks reveals a very prominent 3-fold relationship of the Patterson density around this axis when centred on the origin (Figure 3). The existence of this one 3-fold symmetry axis in the asymmetric unit and the absence of any other such feature in the rest of the unit cell suggests that there is just one trimer per asymmetric unit with its 3-fold symmetry axis running parallel to that found in the Patterson map. This 3-fold symmetry axis will allow phase improvement by real space non-crystallographic symmetry averaging of the electron density map (Bricogne, 1976).

We thank David Stevens and Janet Newman for excellent technical assistance. F.M.H. acknowledges support from the Helen Hay Whitney Foundation and the *Howard Hughes Medical Institute. Support for this work* was from NIH grant AI-13654. D.C.W. is an investigator of the Howard Hughes Medical Institute.

References

Blum, M., Metcalf, P., Harrison, S. C. & Wiley, D. C. (1987). A system for collection and on-line integration of X-ray diffraction data from a multiwire area detector. *J. Appl. Crystallogr.* **20**, 235–242.

Bricogne, G. (1976). Methods and programs for direct-space exploitation of geometric redundancies. *Acta Crystallogr. sect. A*, **32**, 832–847.

Carter, C. W., Jr & Carter, C. W. (1979). Protein crystallization using incomplete factorial experiments. *J. Biol. Chem.* **254**, 12219–12223.

Daniels, R. S., Douglas, A. R. & Skehel, J. J. (1983). Analyses of the antigenicity of influenza haemagglutinin at the pH optimum for virus-mediated membrane fusion. *J. Gen. Virol.* **64**, 1657–1661.

Daniels, R. S., Downie, J. C., Hay, A. J., Knossow, M., Skehel, J. J., Wang, M. L. & Wiley, D. C. (1985). Fusion mutants of the influenza virus hemagglutinin glycoprotein. *Cell*, **40**, 431–439.

Doms, R. W., Helenius, A. & White, J. (1985). Membrane fusion activity of the influenza virus hemagglutinin. *J. Biol. Chem.* **260**, 2973–2981.

Durbin, R. M., Burns, R., Moulai, J., Metcalf, P., Freymann, D., Blum, M., Anderson, J. E., Harrison, S. C. & Wiley, D. C. (1986). Protein, DNA and virus crystallography with a focussed imaging proportional counter. *Science*, **232**, 1127–1132.

Gamblin, S. J. & Rodgers, D. W. (1993). Some practical details of data collection at 100K. In *Proceedings of the Daresbury Study Weekend on Data Collection* (Sawyer, L., Isaacs, N. & Bailey, S., eds), CCP4, SERC, Daresbury, Warrington.

Godley, L., Pfeifer, J., Steinhauer, D., Ely, B., Shaw, C., Kaufmann, R., Suchanek, E., Pabo, C., Skehel, J. J., Wiley, D. C. & Wharton, S. (1992). Introduction of intersubunit disulfide bonds in the membrane-distal region of the influenza hemagglutinin abolishes membrane fusion activity. *Cell*, **68**, 635–645.

Haas, D. J. & Rossman, M. G. (1970). Crystallographic studies on lactate dehydrogenase at −75°C. *Acta Crystallogr. sect. B*, **26**, 998–1004.

Henderson, R. (1990). Cryo-protection of protein crystals against radiation damage in electron and X-ray diffraction. *Proc. Roy. Soc. ser. B*, **241**, 6–8.

Hope, H. (1988). Cryocrystallography of biological macromolecules, a generally applicable method. *Acta Crystallogr. sect. B*, **44**, 22–26.

Hope, H. (1990). Crystallography of biological macromolecules at ultra-low temperature. *Annu. Rev. Biophys. Chem.* **19**, 107–126.

Huang, R. T. C., Rott, R. & Klenk, H.-D. (1981). Influenza viruses cause hemolysis and fusion of cells. *Virology*, **110**, 243–247.

Jackson, D. C. & Nestorowicz, A. (1985). Antigenic determinants of influenza virus hemagglutinin. *Virology*, **145**, 72–83.

Jancarik, J. & Kim, S. H. (1991). Sparse matrix sampling: a screening method for crystallization of proteins. *J. Appl. Crystallogr.* **24**, 409–411.

Maeda, T. & Ohnshi, S. (1980). Activation of influenza virus by acidic media causes hemolysis and fusion of erythrocytes. *FEBS Letters*, **122**, 283–287.

Matthews, B. W. (1968). Solvent content of protein crystals. *J. Mol. Biol.* **33**, 491–497.

Petsko, G. A. (1975). Protein crystallography at sub-zero temperature, cryo-protective mother liquors for protein crystals. *J. Mol. Biol.* **96**, 381–392.

Ruigrok, R. W. H., Aitken, A., Calder, L. J., Martin, S. R., Skehel, J. J., Wharton, S. A., Weis, W. & Wiley, D. C. (1988). Studies on the structure of the influenza virus haemagglutinin at the pH of membrane fusion. *J. Gen. Virol.* **69**, 2785–2795.

Skehel, J. J., Bayley, P. M., Brown, E. B., Martin, S. R., Waterfield, M. D., White, J. M., Wilson, I. A. & Wiley, D. C. (1982). Changes in the conformation of influenza virus hemagglutinin at the pH optimum of virus-mediated membrane fusion. *Proc. Nat. Acad. Sci., U.S.A.* **79**, 93–97.

Teng, T. Y. (1990). Mounting of crystals for macromolecular crystallography in a free-standing thin film. *J. Appl. Crystallogr.* **23**, 387–391.

Webster, R. G., Brown, L. E. & Jackson, D. C. (1983). Changes in the antigenicity of the hemagglutinin molecule of H3 influenza virus at acidic pH. *Virology*, **126**, 587–599.

White, J. M. & Wilson, I. A. (1987). Anti-peptide antibodies detect steps in a protein conformational change: low-pH activation of the influenza virus hemagglutinin. *J. Cell. Biol.* **105**, 2887–2896.

White, J., Matlin, K. & Helenius, A. (1981). Cell fusion by semliki forest, influenza, and vesicular stomatitis viruses. *J. Cell. Biol.* **89**, 674–679.

Wiley, D. C. & Skehel, J. J. (1977). Crystallization and X-ray diffraction studies of the haemagglutinin glycoprotein from the membrane of influenza virus. *J. Mol. Biol.* **112**, 343–345.

Wiley, D. C. & Skehel, J. J. (1987). The structure and function of the haemagglutinin membrane glycoprotein of influenza virus. *Annu. Rev. Biochem.* **56**, 365–394.

Wilson, I. A., Skehel, J. J. & Wiley, D. C. (1981). Structure of the haemagglutinin membrane glycoprotein of influenza virus at 3 Å resolution. *Nature (London)*, **289**, 366–373.

Yewdell, J. W., Gerhard, W. & Bachi, T. (1983). Monoclonal anti-hemagglutinin antibodies detect irreversible antigenic alterations that coincide with the acid activation of influenza virus A/PR/834-mediated hemolysis. *J. Virol.* **48**, 239–248.

Edited by A. Klug

(Received 18 November 1993; accepted 2 December 1993)